MedChemComm

RESEARCH ARTICLE

View Article Online
View Journal | View Issue

Cite this: *Med. Chem. Commun.*, 2018, **9**, 525

Synthesis, characterization and biological evaluation of six highly cytotoxic ruthenium(II) complexes with 4′-substituted-2,2′:6′,2″-terpyridine†

Qi-Pin Qin, ‡[ac] Ting Meng,‡[ac] Ming-Xiong Tan, *[ac] Yan-Cheng Liu, [c] Shu-Long Wang,*[ac] Bi-Qun Zou *[b] and Hong Liang[c]

Received 20th October 2017,
Accepted 31st January 2018

DOI: 10.1039/c7md00532f

rsc.li/medchemcomm

Herein, six ruthenium(II) terpyridine complexes, *i.e.* [$RuCl_2$(4-EtN-Phtpy)(DMSO)] (**Ru1**), [$RuCl_2$(4-MeO-Phtpy)(DMSO)] (**Ru2**), [$RuCl_2$(2-MeO-Phtpy)(DMSO)] (**Ru3**), [$RuCl_2$(3-MeO-Phtpy)(DMSO)] (**Ru4**), [$RuCl_2$(1-Bip-Phtpy)(DMSO)] (**Ru5**), and [$RuCl_2$(1-Pyr-Phtpy)(DMSO)] (**Ru6**) with 4′-(4-diethylaminophenyl)-2,2′:6′,2″-terpyridine (4-EtN-Phtpy), 4′-(4-methoxyphenyl)-2,2′:6′,2″-terpyridine (4-MeO-Phtpy), 4′-(2-methoxyphenyl)-2,2′:6′,2″-terpyridine (2-MeO-Phtpy), 4′-(3-methoxyphenyl)-2,2′:6′,2″-terpyridine (3-MeO-Phtpy), 4′-(1-biphenylene)-2,2′:6′,2″-terpyridine (1-Bip-Phtpy), and 4′-(1-pyrene)-2,2′:6′,2″-terpyridine (1-Pyr-Phtpy), respectively, were synthesized and fully characterized. The MTT assay demonstrates that the *in vitro* anticancer activity of **Ru1** is higher than that of **Ru2**–**Ru6** and more selective for Hep-G2 cells than for normal HL-7702 cells. In addition, various biological assays show that **Ru1** and **Ru6**, especially the **Ru1** complex, are telomerase inhibitors targeting c-myc G4 DNA and also cause apoptosis of Hep-G2 cells. With the same Ru center, the *in vitro* antitumor activity and cellular uptake ability of the 4-EtN-Phtpy and 1-Bip-Phtpy ligands follow the order 4-EtN-Phtpy > 1-Bip-Phtpy.

Introduction

Recently, a variety of genes such as c-kit-2, POT1, bcl-2, c-myc, and c-kit-1 have been considered as appealing targets for drug intervention in the therapy of many diseases.[1–8] These targets are often associated with human diseases such as HIV, cancer, and diabetes.[1–8] In particular, it is widely accepted that the aberrant over-expression of c-myc is associated with a variety of malignant tumors.[9] In addition, the nuclear hypersensitivity element III_1, upstream of the P1 promoter of c-myc, controls 80–90% of the c-myc transcription level.[10–12] In the past decade, a large number of planar aromatic molecules, such as the natural product telomestatin,[13,14] cationic porphyrins (TMPyP4 or Se2SAP),[15,16] quindolines,[13,17,18] perylenes,[19] and berberine,[13,17,18] have been studied due to their binding and stabilization of the G-quadruplex DNA (G4 DNA) in the NHE III_1 sequence to suppress c-myc transcription in tumor cell lines. Therefore, the inhibition of the transcription of c-myc *via* stabilization of G-quadruplex DNA formation is a promising strategy for the design and development of efficacious anticancer agents.[1–19]

An increasing number of metal complexes, such as Ni(II),[20,21] Pt(II),[22–30] Pd(II),[31] Ru(II),[32] Cu(II),[33] Co(II), and Zn(II)[34] complexes, have been reported recently as G-quadruplex DNA binders. In addition, it has been reported that a series of metal–terpyridine complexes with Zn(II), Ru(II), Cu(II), Pd(II), iridium(III), and Pt(II) ion centers can act as effective G4-DNA ligands.[31,35–45] For example, Ang and co-workers designed four dinuclear platinum(II)–terpyridine complexes and showed that they acted as efficient G4-DNA ligands with high selectivity (ΔT_m up to 17.0 °C) over duplex DNA (ΔT_m = 1.0 °C).[43] A dinuclear copper(II)–terpyridine complex has been reported to bind to G4 DNA with high affinity and stabilize the antiparallel topology, and its selectivity for G4 is 100-fold higher than that for duplex DNA.[35,44,45] Bertrand and co-workers also designed a range of copper–

[a] *Guangxi Key Laboratory of Agricultural Resources Chemistry and Biotechnology, College of Chemistry and Food Science, Yulin Normal University, 1303 Jiaoyudong Road, Yulin 537000, PR China. E-mail: mxtan2018@126.com, shulonghs@163.com; Fax: +86 775 2623650; Tel: +86 775 2623650*

[b] *Department of Chemistry, Guilin Normal College, 21 Xinyi Road, Gulin 541001, PR China. E-mail: zoubiqun@163.com*

[c] *State Key Laboratory for the Chemistry and Molecular Engineering of Medicinal Resources, School of Chemistry and Pharmacy, Guangxi Normal University, 15 Yucai Road, Guilin 541004, PR China*

† Electronic supplementary information (ESI) available: Vendor codes for the tested compounds, ^{1}H NMR, ESI-MS, IR, ^{13}C NMR, UV-vis data and crystal data. CCDC no. 1563746 for **Ru5** contains the supplementary crystallographic data for this study. For ESI and crystallographic data in CIF or other electronic format see DOI: 10.1039/c7md00532f

‡ These authors contributed equally to this work.

terpyridine complexes, which displayed higher affinity and selectivity for G4 DNA than other complexes.[35,36] However, Ru(II) complexes with 4′-substituted-2,2′:6′,2″-terpyridine have been rarely studied, and detailed studies on their molecular mechanisms of action are still lacking.[46–52]

In this study, we designed and synthesized six ruthenium(II) terpyridine complexes: [$RuCl_2$(4-EtN-Phtpy)(DMSO)] (**Ru1**), [$RuCl_2$(4-MeO-Phtpy)(DMSO)] (**Ru2**), [$RuCl_2$(2-MeO-Phtpy)(DMSO)] (**Ru3**), [$RuCl_2$(3-MeO-Phtpy)(DMSO)] (**Ru4**), [$RuCl_2$(1-Bip-Phtpy)(DMSO)] (**Ru5**), and [$RuCl_2$(1-Pyr-Phtpy)(DMSO)] (**Ru6**) with 4′-(4-diethylaminophenyl)-2,2′:6′,2″-terpyridine (4-EtN-Phtpy), 4′-(4-methoxyphenyl)-2,2′:6′,2″-terpyridine (4-MeO-Phtpy), 4′-(2-methoxyphenyl)-2,2′:6′,2″-terpyridine (2-MeO-Phtpy), 4′-(3-methoxyphenyl)-2,2′:6′,2″-terpyridine (3-MeO-Phtpy), 4′-(1-biphenylene)-2,2′:6′,2″-terpyridine (1-Bip-Phtpy), and 4′-(1-pyrene)-2,2′:6′,2″-terpyridine (1-Pyr-Phtpy), respectively. These six Ru(II) complexes exhibit remarkable and different *in vitro* cytotoxicities, which also exert inhibitory effects on the telomerase activity by directly targeting c-myc promoter elements (c-myc G4 DNA).

Results and discussion

Synthesis

The six ligands 4-EtN-Phtpy, 4-MeO-Phtpy, 2-MeO-Phtpy, 3-MeO-Phtpy, 1-Bip-Phtpy, and 1-Pyr-Phtpy were synthesized according to the procedures reported by Li *et al.*[53] The title complexes **Ru1**, **Ru2**, **Ru3**, **Ru4**, **Ru5**, and **Ru6** were prepared *via* the reaction of *cis*-Ru(DMSO)$_4$$Cl_2$ with 4-EtN-Phtpy, 4-MeO-Phtpy, 2-MeO-Phtpy, 3-MeO-Phtpy, 1-Bip-Phtpy, and 1-Pyr-Phtpy, respectively, in a 90% (v/v) methanol–water solution (Scheme 1). The complexes **Ru1**–**Ru6** were characterized *via* elemental analysis, ^{1}H and ^{13}C NMR spectroscopy, ^{1}H–^{1}H COSY NMR spectra, IR spectroscopy, UV-vis spectroscopy, single-crystal X-ray diffraction analysis, and ESI-MS (Fig. S1–S40, Table S4†).

Crystal structure characterization

The single crystal X-ray analysis revealed that **Ru5** crystallized as a monoclinic crystal system with the $P2_1/c$ space group. As shown in Fig. 1, the central Ru(II) in **Ru5** is six-coordinated by

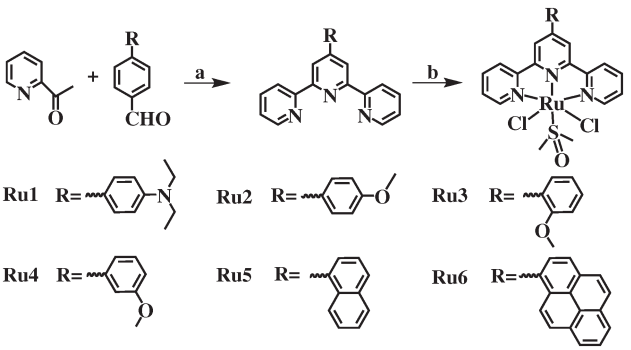

Scheme 1 Synthetic routes for **Ru1**–**Ru6** with 4′-substituted-2,2′:6′,2″-terpyridine. Reagents and solvents are as follows: (a) ethanol, KOH, 25% NH_3 (aq) and (b) *cis*-Ru(DMSO)$_4$$Cl_2$ (0.1 mmol, 0.0485 g), CH_3OH : H_2O (v : v = 9 : 1), 80 °C.

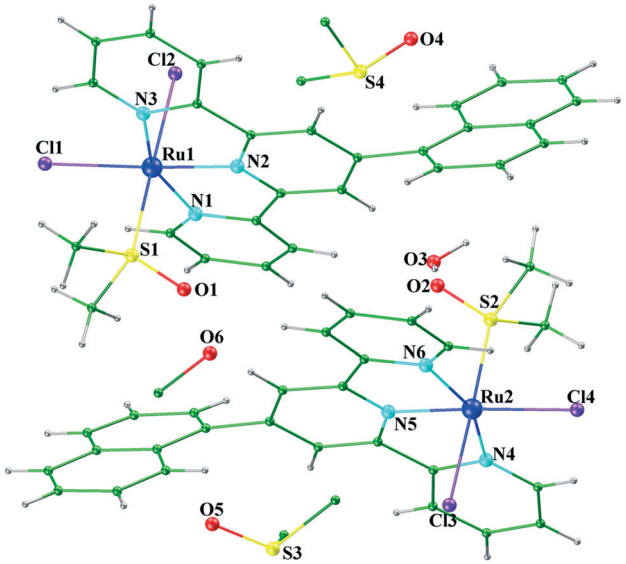

Fig. 1 ORTEP view of the molecular structure of **Ru5**. Thermal ellipsoids for non-hydrogen atoms are drawn at a 30% probability level.

two chlorides, one bidentate chelating big planar ligand *N*′*N*′*N*-1-Bip-Phtpy, and one DMSO, adopting a distorted octahedral geometry. In addition, the Ru–Cl, Ru–N, and Ru–S bond lengths are in the range of 2.4175(14)–2.4440(14), 1.949(4)–2.081(5), and 2.2184(15)–2.2190(16) Å, respectively, which are within the normal range. The bite angles (N1–Ru1–Cl2 and N1–Ru1–Cl1) of the chelate ring are 87.03(13) and 102.66(12)°, respectively, which are smaller than the S1–Ru1–Cl2 bite angles (177.92(6)°). The details of the selected bond lengths for **Ru5** are tabulated in Table S2,† and the structural refinement parameters and crystallographic data are summarized in Tables S1 and S3,† respectively.

Stability of Ru1–Ru6 in TBS

Ru1–**Ru6** were tested for their stability in 10 mM TBS (Tris-HCl buffer solution 10 mM, pH 7.35, containing 2.0% DMSO) *via* UV-vis spectroscopy. As shown in Fig. S41 and Table S5,† no obvious spectral changes were observed in the UV-vis spectra of **Ru1**–**Ru6** for 48 h at 37 °C; this demonstrated that they were also stable in their coordinating mode in TBS. These results confirm that the six complexes **Ru1**–**Ru6** (2.0×10^{-5} M) are stable under physiologically relevant conditions for 48 h, which ensure adequate cellular uptake of **Ru1**–**Ru6** during the time course of the MTT assay.

In vitro cytotoxicity

The *in vitro* cytotoxic activities of the six ligands 4-EtN-Phtpy, 4-MeO-Phtpy, 2-MeO-Phtpy, 3-MeO-Phtpy, and 1-Bip-Phtpy,1-Pyr-Phtpy, **Ru1**–**Ru6**, cisplatin, and *cis*-Ru(DMSO)$_4$$Cl_2$ against the BEL-7404, Hep-G2, HL-7702, NCI-H460, and MGC80-3 cell lines were assessed using the MTT assay. The concentrations of these compounds ranged from 1.25 μM to 20.0 μM. As shown in Tables 1 and S6,† the inhibitory rates of **Ru1**–**Ru6** against the

Table 1 IC_{50}[a] (μM) values of 4′-substituted-2,2′:6′,2″-terpyridine, **Ru1**–**Ru6**, and cisplatin towards the five selected cell lines after incubation for 48 h

Compd.	BEL-7404	Hep-G2	NCI-H460	MGC80-3	HL-7702[c]
4-EtN-Phtpy	26.18 ± 0.95	19.12 ± 1.39	16.54 ± 1.61	13.62 ± 0.51	38.02 ± 1.95 (1.99)
Ru1	2.89 ± 0.66	1.28 ± 0.44	3.56 ± 1.60	6.01 ± 1.68	31.18 ± 1.19 (24.94)
4-MeO-Phtpy	56.78 ± 0.65	28.43 ± 0.39	33.78 ± 1.76	35.71 ± 0.92	18.11 ± 1.07 (0.64)
Ru2	19.26 ± 1.20	10.19 ± 1.01	16.08 ± 1.06	15.01 ± 1.44	21.17 ± 1.88 (2.08)
2-MeO-Phtpy	36.94 ± 0.80	26.40 ± 1.45	24.73 ± 1.10	23.02 ± 1.44	17.16 ± 1.03 (0.65)
Ru3	17.54 ± 0.63	7.35 ± 0.59	9.34 ± 1.85	11.18 ± 0.62	16.89 ± 0.57 (2.30)
3-MeO-Phtpy	34.34 ± 1.02	19.67 ± 0.73	19.96 ± 0.35	20.96 ± 0.31	35.11 ± 0.81 (1.78)
Ru4	10.17 ± 1.45	6.04 ± 0.94	8.89 ± 0.75	10.78 ± 1.47	40.16 ± 1.51 (6.65)
1-Bip-Phtpy	30.56 ± 0.53	19.98 ± 1.02	19.42 ± 1.56	18.45 ± 1.32	25.16 ± 1.34 (1.26)
Ru5	8.52 ± 0.75	4.89 ± 1.49	6.72 ± 0.40	9.96 ± 0.59	35.21 ± 1.05 (7.20)
1-Pyr-Phtpy	45.12 ± 1.74	19.47 ± 1.23	17.43 ± 1.04	16.18 ± 0.69	30.02 ± 1.19 (1.54)
Ru6	5.09 ± 0.40	3.01 ± 0.91	5.89 ± 1.58	7.79 ± 1.43	27.56 ± 0.81 (9.16)
Cisplatin[b]	16.91 ± 1.01	18.68 ± 0.67	18.01 ± 1.23	13.99 ± 0.76	17.98 ± 1.94 (0.96)

[a] IC_{50} values are presented as the mean ± SD (standard error of the mean) from six independent experiments. [b] Cisplatin was dissolved at a concentration of 1.0 mM in 0.154 M NaCl.[57] [c] The selectivity index factor, defined as IC_{50} (HL-7702 normal cells)/IC_{50} (Hep-G2 tumor cells), is given in parentheses.[54–56]

tested cancer cells were higher than those of 4-EtN-Phtpy, 4-MeO-Phtpy, 2-MeO-Phtpy, 3-MeO-Phtpy, 1-Bip-Phtpy, 1-Pyr-Phtpy, and *cis*-Ru(DMSO)$_4$Cl$_2$. Importantly, **Ru1** exhibited higher *in vitro* cytotoxicity against all the selected cancer cell lines than 4-EtN-Phtpy, 4-MeO-Phtpy, 2-MeO-Phtpy, 3-MeO-Phtpy, 1-Bip-Phtpy, 1-Pyr-Phtpy, and **Ru2**–**Ru6**, but relatively higher cytotoxicity than cisplatin, a widely used clinical antitumor drug. Overall, **Ru1**–**Ru6** were more sensitive to Hep-G2 tumor cells and exhibited lower IC_{50} values on Hep-G2 cells with 1.28 ± 0.44, 10.19 ± 1.01, 7.35 ± 0.59, 6.04 ± 0.94, 4.89 ± 1.49, and 3.01 ± 0.91 μM values for **Ru1**, **Ru2**, **Ru3**, **Ru4**, **Ru5**, and **Ru6**, respectively. The different *in vitro* antitumor activities of **Ru1**–**Ru6** against the tested cancer cells are related to 4′-substituted-2,2′:6′,2″-terpyridine in the following order: 4-EtN-Phtpy > 1-Pyr-Phtpy > 1-Bip-Phtpy > 3-MeO-Phtpy > 2-MeO-Phtpy > 4-MeO-Phtpy. Compared with their toxicity towards cancer cells, **Ru1**–**Ru6** were considerably less toxic towards the normal HL-7702 cells, with the IC_{50} values ranging from 21.17 ± 1.88 μM to more than 40.16 ± 1.51 μM, which were significantly higher than that of cisplatin (17.98 ± 1.94 μM). Remarkably, the cytotoxicities of **Ru1**–**Ru6** against the Hep-G2 cells and HL-7702 cells (human normal cells) were characterized by remarkably high selectivity index factors of more than 3.0 (Table 1).[54–56] **Ru1** and **Ru6** showed the best selectivity indices (highest selectivity index factor values) of 22.94 and 9.16, higher than those of 4-EtN-Phtpy, 4-MeO-Phtpy, 2-MeO-Phtpy, 3-MeO-Phtpy, 1-Bip-Phtpy, 1-Pyr-Phtpy, **Ru2**–**Ru5**, and cisplatin; this indicated the high selectivity of **Ru1** and **Ru6** for Hep-G2 cells. In addition, the MTT assay indicated that Hep-G2 cells exhibited higher selectivity for **Ru1** and **Ru6** than for other compounds; therefore, **Ru1** and **Ru6** were selected for the cellular uptake assay, apoptosis analysis, western blot, transfection assay, and RT-PCR in the Hep-G2 cells.

Ruthenium accumulation and distribution in Hep-G2 cells

To investigate whether the nuclear fraction or/and mitochondria fraction plays a role in the cellular accumulation of Ru metal, Hep-G2 cells have been incubated with **Ru1** (1.3 μM) and **Ru6** (3.0 μM). The uptakes and distributions of **Ru1** (1.3 μM) and **Ru6** (3.0 μM) in the Hep-G2 cells were studied in more detail using the method reported by Sadler, Chen, Liu, and Schreiber.[58–61] At first, the total cellular accumulation of Ru from **Ru1** (1.3 μM) and **Ru6** (3.0 μM) was determined for Hep-G2 cells using the ICP-MS assay. Ru accumulation after 24 h of exposure under 5% CO_2 was higher for **Ru1** ((5.32 ± 0.15 ng Ru)/10^6 cells) than for **Ru6** ((3.67 ± 0.24 ng Ru)/10^6 cells) and cisplatin (10.0 μM) in the Hep-G2 cells (Fig. 2A).[58] In addition, Fig. 2B showed that the Ru accumulation for **Ru1** (1.3 μM) and **Ru6** (3.0 μM) reached a high level in the nuclear fraction and mitochondrial fraction, whereas cisplatin was only accumulated in the mitochondrial membrane fraction.[58,61]

Telomerase inhibition

To examine the ability of **Ru1** (1.3 μM) and **Ru6** (3.0 μM) to inhibit the telomerase activity, the TRAP assay was performed.[62–66] Fig. 3 clearly reveals that **Ru1** (1.3 μM) exhibits greater telomerase inhibitory activity (inhibitory rate of 53.06%) than **Ru6** (3.0 μM, inhibitory rate of 16.34%) and cisplatin (10.0 μM, inhibitory rate of 17.89%)[58] in the Hep-G2 cells. Herein, one of the notable features was the variation

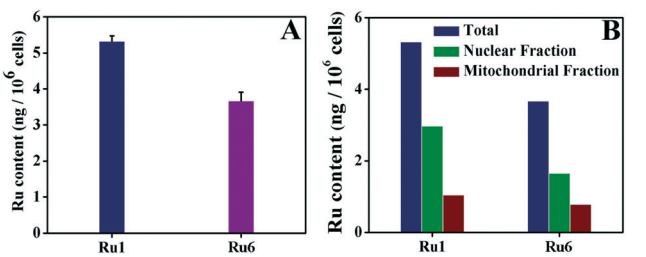

Fig. 2 Accumulation of Ru in the Hep-G2 cells after incubation with **Ru1** (1.3 μM) and **Ru6** (3.0 μM) for 24 h at 37 °C. The total Ru content in the whole Hep-G2 cell (A) and in different fractions (B) was measured by ICP-MS.

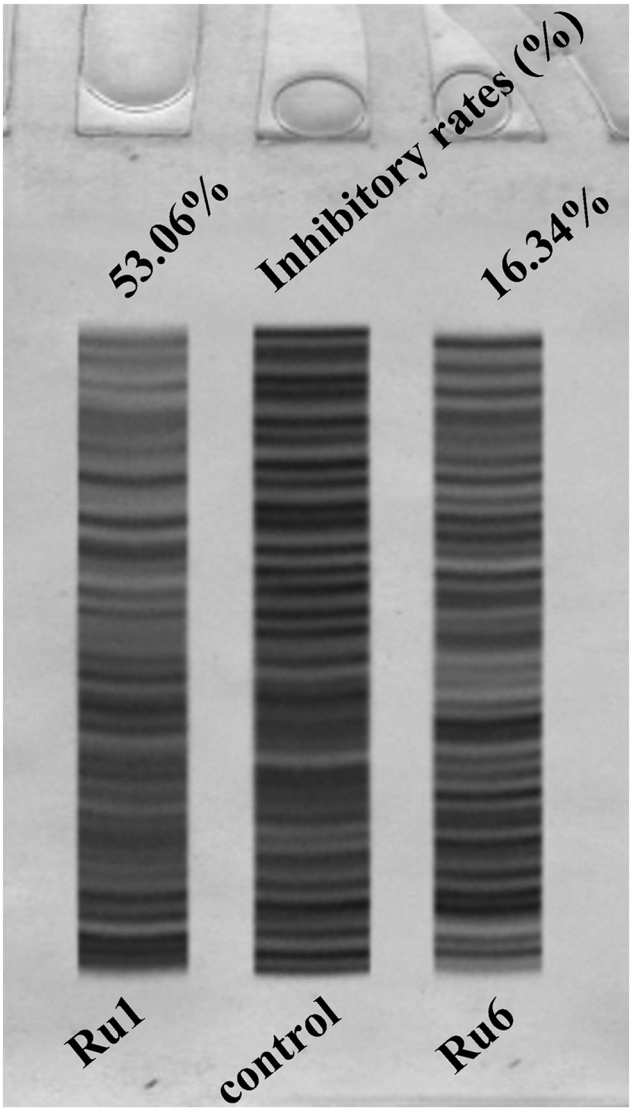

Fig. 3 Influence of **Ru1** (1.3 μM) and **Ru6** (3.0 μM) on the telomerase activity of Hep-G2 cells for 24 h.

with different ligands (4-EtN-Phtpy > 1-Bip-Phtpy), which might contribute to their telomerase inhibitory activity and other antitumour actions.

Inhibition of hTERT and c-myc gene and protein expression by Ru1 and Ru2

Many groups have carried out research to identify or design c-myc G4-ligands, which specifically bind to the G4-DNA and inhibit cell proliferation.[67–70] It is important to know whether c-myc and hTERT are involved in the inhibition of telomerase activity by **Ru1** (1.3 μM) and **Ru6** (3.0 μM) in the Hep-G2 cancer cells. Thus, we performed RT-qPCR analysis and Western blot assay using Hep-G2 tumor cells. As shown in Fig. 4 and 5, **Ru1** (1.3 μM) was more active in inhibiting hTERT and c-myc gene and protein expression level than **Ru6** (3.0 μM) and cisplatin (10.0 μM) in the Hep-G2 cells.[58,61] In addition,

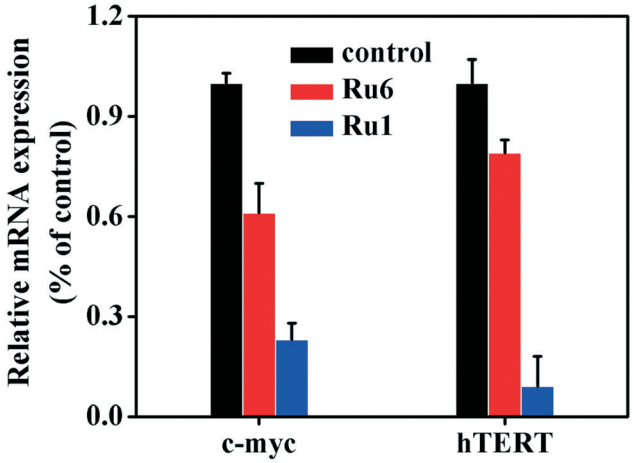

Fig. 4 mRNA expression of the c-myc and hTERT genes after 24 h incubation of the Hep-G2 cells treated with **Ru1** (1.3 μM) and **Ru6** (3.0 μM), determined using the qRT-PCR assay.

the results show different effects on the c-myc and hTERT promoter in the following order: **Ru1** > **Ru6**, consistent with the *in vitro* cytotoxicity (MTT assay), telomerase inhibition, and cell uptake assay results.

Transfection

The binding ability of **Ru1** to G-quadruplex DNAs and duplex DNA was studied using the FID assay and ESI-MS analysis.[8,58,71] As shown in Fig. S42,† the FID assay results indicate that **Ru1** exhibits better selectivity for Pu27 G-quadruplex DNAs (c-myc promoter) than for other DNAs, which are the most efficient TO displacers ($^{Pu27}DC_{50}$ as low as 0.88 μM with **Ru1**). As expected, the selectivity of **Ru1** for G4-DNA over duplex DNA is moderate. Furthermore, to verify further whether **Ru1** (1.3 μM) and **Ru6** (3.0 μM) could directly interact with the c-myc promoter (Pu27 G4 DNA) and regulate the expression of hTRET in Hep-G2 cells, transfection of EGFP (enhanced green fluorescent protein) and c-myc gene vectors into these cells was carried out.[8,58,71–74] After the successful transfection of the c-myc gene vectors in the HepG2 cells, **Ru1** (1.3 μM) and **Ru6** (3.0 μM) were added to the cells and incubated for 24 h and examined *via* fluorescence microcopy or the luciferase reporter gene assay.[58,61] The transfection assay showed that the HepG2 cells emitted green

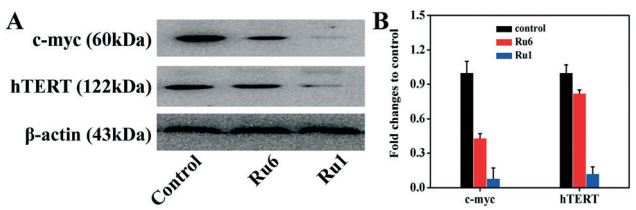

Fig. 5 (A) Protein expression of hTERT, β-actin, and c-myc proteins in the Hep-G2 tumor cells treated with **Ru1** (1.3 μM) and **Ru6** (3.0 μM), analyzed by Western blotting. (B) Densitometric analysis of hTERT or c-myc protein normalized with β-actin. The relative expression of each protein is represented by the ratio of the protein band density to the β-actin band.

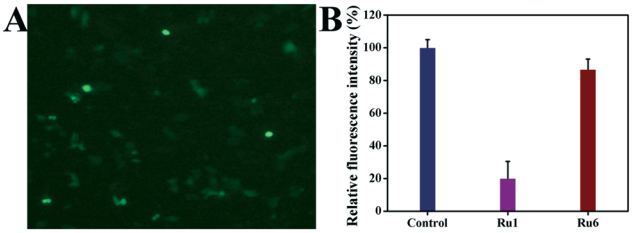

Fig. 6 (A) Successful transfection of EGFP plasmid vector in the HepG2 cells for 6 h. (B) The treatment of Hep-G2 cells with **Ru1** (1.3 μM) and **Ru6** (3.0 μM) for 24 h after 6 h of transfection from 2.0 μg c-myc plasmid by Lipofectamine 2000 (Invitrogen), which showed a significant reduction in green fluorescence emission when they were examined using a multimode plate reader with the luciferase reporter gene assay kit.

fluorescence after EGFP plasmid transfection; this suggested that the transfection was successful (Fig. 6A). These cells were then transfected by c-myc plasmid and treated with **Ru1** (1.3 μM) and **Ru6** (3.0 μM). Consequently, a remarkable decrease in the emission of the bright green fluorescence was observed (Fig. 6B).[58,61] As a result, the treatment of **Ru1** (1.3 μM) reduced the fluorescence emission by 79.82%, whereas the treatment with **Ru6** (3.0 μM) and cisplatin (10.0 μM) only reduced the fluorescence emission by 13.11% and 30.13%, respectively, under the same conditions.[58,61] These results further demonstrate the higher activity of **Ru1** (1.3 μM) to inhibit telomerase activity by directly down-regulating the c-myc promoter (c-myc/Pu27 G4 DNA) in the Hep-G2 cells.

Apoptosis assay by flow cytometry

To determine the percentage of Hep-G2 cells undergoing apoptosis after treatment with **Ru1** (1.3 μM) and **Ru6** (3.0 μM) for 24 h, cell apoptosis analyses using flow cytometry were performed after staining the Hep-G2 cells with Annexin-V-FITC and propidium iodide (PI).[58,61,75] After treatment with **Ru1** (1.3 μM) and **Ru6** (3.0 μM) for 24 h, the percentage of apoptotic cells (Q2 + Q3) increased from 2.22% to 38.60% and 29.00%, and the percentage of early apoptotic Hep-G2 cells was 14.90% and 12.70%, respectively (Fig. 7). Overall, these results indicate that **Ru1**, even at a low concentration of 1.3 μM, could also cause more cell apoptosis than **Ru6** (3.0 μM) and cisplatin (10.0 μM, *ca.* 13.60%) in the HepG2 cells.[32,35]

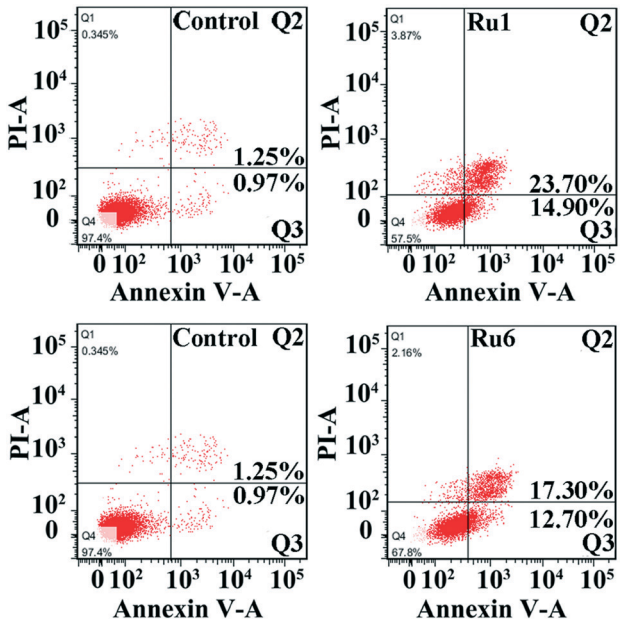

Fig. 7 Cell apoptosis induction in HepG2 cells treated with **Ru1** (1.3 μM) and **Ru6** (3.0 μM) for 24 h.

Conclusions

In this study, six ruthenium(II) terpyridine complexes **Ru1**, **Ru2**, **Ru3**, **Ru4**, **Ru5**, and **Ru6** with 4-EtN-Phtpy, 4-MeO-Phtpy, 2-MeO-Phtpy, 3-MeO-Phtpy, 1-Bip-Phtpy, and 1-Pyr-Phtpy, respectively, were synthesized and fully characterized. **Ru1** showed higher *in vitro* cytotoxicity than **Ru2**–**Ru6**, 4-EtN-Phtpy, 4-MeO-Phtpy, 2-MeO-Phtpy, 3-MeO-Phtpy, 1-Bip-Phtpy, 1-Pyr-Phtpy, and cisplatin on Hep-G2 cells under the same conditions. Various biological assays revealed that **Ru1** acted as a telomerase inhibitor targeting the c-myc G-quadruplex DNA and thus driving the Hep-G2 cells towards apoptosis. Importantly, this study demonstrated a novel class of potent c-myc G4 DNA signaling telomerase inhibitors.

Experimental methods

Synthesis

Synthesis of ligands. Synthesis of 4-EtN-Phtpy, 4-MeO-Phtpy, 2-MeO-Phtpy, 3-MeO-Phtpy, 1-Bip-Phtpy, and 1-Pyr-Phtpy was performed as reported by Li *et al.*[53] Typically, 2.61 mL of 2-acetylpyridine (2.813 g, 23.2 mmol, 2 equiv.) was added to a solution of 4′-substituted benzaldehyde (11.6 mmol, 1 equiv.) in 50 mL of ethanol. Then, KOH pellets (2.6 g, 85%, 46.5 mmol, 4 equiv.) were added to this solution. The reaction was stirred at RT for 10 min. Subsequently, 40 mL of 25% aq. NH_3 was added to the flask dropwise. After 24 h of stirring at 34 °C, 5 mL of 25% aq. NH_3 was added to the reaction mixture again. The flask was cooled to −20 °C, and then, the white precipitate was filtered and washed with cold ethanol. We further purified the ligands by subsequent recrystallization from ethanol–H_2O. Each ligand was recovered by filtration, washed with cold ethanol and petroleum ether, and dried under high vacuum for 24 h (Scheme 1).

Data for 4-EtN-Phtpy. The white product of 4-EtN-Phtpy was suitable for structural characterization. Yield (44.21%). ESI-MS *m/z*: 783.5 $[2M + Na]^+$, *m/z*: 403.2 $[M + Na]^+$. ^1H NMR (500 MHz, DMSO-d_6) δ 8.76 (d, J = 4.3 Hz, 2H), 8.65 (d, J = 6.2 Hz, 4H), 8.02 (t, J = 7.7 Hz, 2H), 7.77 (d, J = 8.8 Hz, 2H), 7.51 (s, 2H), 6.83 (d, J = 8.9 Hz, 2H), 3.43 (s, 4H), 1.14 (s, 6H). Elemental analysis calcd (%) for $C_{25}H_{24}N_4$: C 78.92, H 6.36, N 14.73; found: C 78.89, H 6.38, N 14.70.

Data for 4-MeO-Phtpy. The white product of 4-MeO-Phtpy was suitable for structural characterization. Yield (45.62%). ESI-MS *m/z*: 701.4 $[2M + Na]^+$, *m/z*: 362.1 $[M + Na]^+$. ^1H NMR

(500 MHz, DMSO-d_6) δ 8.75 (d, J = 4.7 Hz, 2H), 8.65 (d, J = 9.1 Hz, 4H), 8.02 (t, J = 7.7 Hz, 2H), 7.87 (d, J = 8.8 Hz, 2H), 7.51 (s, 2H), 7.12 (d, J = 8.8 Hz, 2H), 3.84 (s, 3H). Elemental analysis calcd (%) for $C_{22}H_{17}N_3O$: C 77.86, H 5.05, N 12.38; found: C 77.89, H 5.07, N 12.33.

Data for 2-MeO-Phtpy. The yellow product of 2-MeO-Phtpy was suitable for structural characterization. Yield (45.62%). ESI-MS m/z: 701.4 $[2M + Na]^+$, m/z: 362.1 $[M + Na]^+$. ^{1}H NMR (500 MHz, DMSO-d_6) δ 8.74 (d, J = 4.7 Hz, 2H), 8.67 (d, J = 7.9 Hz, 2H), 8.57 (s, 2H), 8.03 (t, J = 7.7 Hz, 2H), 7.51 (s, 4H), 7.23 (d, J = 8.0 Hz, 1H), 7.14 (s, 1H), 3.84 (s, 3H). Elemental analysis calcd (%) for $C_{22}H_{17}N_3O$: C 77.86, H 5.05, N 12.38; found: C 77.84, H 5.08, N 12.34.

Data for 3-MeO-Phtpy. The white product of 3-MeO-Phtpy was suitable for structural characterization. Yield (45.62%). ESI-MS m/z: 701.4 $[2M + Na]^+$, m/z: 362.1 $[M + Na]^+$. ^{1}H NMR (500 MHz, DMSO-d_6) δ 8.76 (d, J = 4.6 Hz, 2H), 8.66 (d, J = 8.9 Hz, 4H), 8.03 (t, J = 7.7 Hz, 2H), 7.52 (s, 2H), 7.50 (d, J = 7.9 Hz, 1H), 7.45 (d, J = 7.8 Hz, 1H), 7.39 (s, 1H), 7.11 (d, J = 7.4 Hz, 1H), 3.88 (s, 3H). Elemental analysis calcd (%) for $C_{22}H_{17}N_3O$: C 77.86, H 5.05, N 12.38; found: C 77.81, H 5.10, N 12.35.

Data for 1-Bip-Phtpy. The yellow product of 1-Bip-Phtpy was suitable for structural characterization. Yield (40.11%). ESI-MS m/z: 741.4 $[2M + Na]^+$, m/z: 382.1 $[M + Na]^+$. ^{1}H NMR (500 MHz, DMSO-d_6) δ 8.74 (d, J = 7.9 Hz, 2H), 8.71 (d, J = 5.4 Hz, 2H), 8.55 (s, 2H), 8.09 (s, 2H), 8.05 (d, J = 7.8 Hz, 2H), 7.91 (d, J = 8.4 Hz, 1H), 7.67 (d, J = 7.3 Hz, 2H), 7.63–7.55 (m, 2H), 7.54–7.50 (m, 2H). Elemental analysis calcd (%) for $C_{25}H_{17}N_3$: C 83.54, H 4.77, N 11.69; found: C 83.50, H 4.80, N 11.66.

Data for 1-Pyr-Phtpy. The yellow product of 1-Pyr-Phtpy was suitable for structural characterization. Yield (46.98%). ESI-MS m/z: 889.4 $[2M + Na]^+$, m/z: 456.2 $[M + Na]^+$. ^{1}H NMR (500 MHz, DMSO-d_6) δ 8.79 (d, J = 7.9 Hz, 2H), 8.74 (d, J = 4.6 Hz, 2H), 8.71 (s, 2H), 8.48 (d, J = 7.8 Hz, 1H), 8.40 (d, J = 7.7 Hz, 1H), 8.35 (d, J = 7.3 Hz, 1H), 8.31 (s, 2H), 8.27 (d, J = 9.3 Hz, 1H), 8.23 (d, J = 2.7 Hz, 1H), 8.15 (s, 2H), 8.09 (t, J = 6.9 Hz, 2H), 7.57–7.53 (m, 2H). Elemental analysis calcd (%) for $C_{31}H_{19}N_3$: C 88.89, H 4.42, N 9.69; found: C 88.93, H 4.39, N 9.61.

Synthesis of Ru1–Ru6. *cis*-Ru(DMSO)$_4$Cl$_2$ (0.0485 g, 0.1 mmol), 0.1 mmol 4-EtN-Phtpy, 4-MeO-Phtpy, 2-MeO-Phtpy, 3-MeO-Phtpy, 1-Bip-Phtpy or 1-Pyr-Phtpy, 0.10 mL H_2O, and 0.90 mL CH_3OH, were placed in a 25.0 cm long Pyrex tube that was then quenched in liquid N_2 before being evacuated and sealed, which was then heated at 80 °C for three days. The resulting black products suitable for structural characterization were isolated, washed with ethanol and ether, and air-dried.

*Data for **Ru1**.* The black product of **Ru1** was suitable for structural characterization. Yield (0.0564 g, 89.50%). ESI-MS m/z: 862.4 $[M - Cl + 3DMSO + CH_3OH]^+$. ^{1}H NMR (600 MHz, DMSO-d_6) δ 9.35 (d, J = 5.4 Hz, 2H), 8.87 (s, 2H), 8.79 (d, J = 8.0 Hz, 2H), 8.12 (d, J = 8.9 Hz, 2H), 7.99 (d, J = 1.2 Hz, 2H), 7.51 (s, 2H), 6.88 (d, J = 9.0 Hz, 2H), 3.49 (d, J = 7.0 Hz, 4H), 2.54 (s, 6H), 1.18 (t, J = 7.0 Hz, 6H). ^{13}C NMR (151 MHz, DMSO-d_6) δ 159.26, 156.76, 148.85, 147.97, 136.59, 128.78, 126.08, 123.16, 121.76, 116.89, 116.51, 111.48, 43.76, 40.43, 40.05, 39.93, 39.79, 39.65, 39.51, 39.38, 39.24, 39.10, 12.53. IR (KBr): 3573, 3405, 2973, 2920, 1592, 1532, 1469, 1419, 1355, 1254, 1220, 1158, 1077, 1044, 1010, 925, 888, 826, 756, 789, 726, 676, 517, 455, 430 cm^{-1}. Elemental analysis calcd (%) for $C_{27}H_{30}Cl_2N_4ORuS$: C 51.43, H 4.80, N 8.88; found: C 51.40, H 4.85, N 8.84. In addition, the ^{1}H–^{1}H COSY cross-peaks (Fig. S34–S40†) of H-4/H-3/H-2 and H-2/H-1 indicated the presence of a carbon chain C-4–C-3–C-2–C-1 in **Ru1**. Similarity, the carbon chains C-4′–C-3′–C-2′–C-1′, C-11–C-12, C-14–C-15, C-17–C-18, and C-19–C-20 were observed in **Ru1**.

*Data for **Ru2**.* The black product of **Ru2** was suitable for structural characterization. Yield (0.0501 g, 85.00%). ESI-MS m/z: 780.2 $[M - Cl + 2DMSO + CH_3CN + CH_3OH]^+$. ^{1}H NMR (600 MHz, DMSO-d_6) δ 9.36 (d, J = 5.4 Hz, 2H), 8.96 (s, 2H), 8.81 (d, J = 7.9 Hz, 2H), 8.24 (d, J = 8.7 Hz, 2H), 8.01 (t, J = 7.7 Hz, 2H), 7.54 (t, J = 6.5 Hz, 2H), 7.23 (d, J = 8.7 Hz, 2H), 3.91 (s, 3H), 3.60 (s, 2H), 2.54 (s, 6H). ^{13}C NMR (151 MHz, DMSO-d_6) δ 160.98, 159.01, 157.11, 155.69, 147.29, 136.67, 129.14, 128.44, 126.28, 123.36, 118.15, 114.64, 55.48, 44.61, 40.43, 40.05, 39.93, 39.79, 39.65, 39.52, 39.38, 39.24, 39.10. IR (KBr): 3452, 2999, 2919, 2835, 1601, 1524, 1468, 1435, 1411, 1300, 1271, 1247, 1195, 1078, 1053, 1026, 1005, 961, 884, 825, 787, 756, 728, 677, 594, 528, 427 cm^{-1}. Elemental analysis calcd (%) for $C_{24}H_{23}Cl_2N_3O_2RuS$: C 48.90, H 3.93, N 7.13; found: C 48.87, H 3.95, N 7.11.

*Data for **Ru3**.* The black product of **Ru3** was suitable for structural characterization. Yield (0.0471 g, 80.00%). ESI-MS m/z: 780.2 $[M - Cl + 2DMSO + CH_3CN + CH_3OH]^+$. ^{1}H NMR (600 MHz, DMSO-d_6) δ 9.37 (d, J = 5.5 Hz, 2H), 8.78 (s, 2H), 8.65 (d, J = 7.9 Hz, 2H), 7.97 (dd, J = 12.1, 4.5 Hz, 2H), 7.72 (dd, J = 7.5, 1.5 Hz, 1H), 7.54 (dt, J = 13.5, 7.2 Hz, 3H), 7.31 (d, J = 8.4 Hz, 1H), 7.22 (t, J = 7.4 Hz, 1H), 3.93 (s, 3H), 3.61 (s, 2H), 2.52 (m, 6H). ^{13}C NMR (151 MHz, DMSO-d_6) δ 158.93, 156.58, 156.52, 155.69, 146.17, 136.81, 131.11, 130.89, 126.31, 123.16, 121.89, 121.01, 111.97, 55.83, 44.59, 40.43, 39.93, 39.79, 39.65, 39.52, 39.38, 39.24, 39.10. IR (KBr): 3854, 3433, 3048, 3014, 2927, 2836, 1608, 1496, 1469, 1416, 1294, 1250, 1066, 1047, 1016 888, 791, 759, 678, 633, 465, 429 cm^{-1}. Elemental analysis calcd (%) for $C_{24}H_{23}Cl_2N_3O_2RuS$: C 48.90, H 3.93, N 7.13; found: C 48.93, H 3.90, N 7.10.

*Data for **Ru4**.* The black product of **Ru4** was suitable for structural characterization. Yield (0.0530 g, 90.00%). ESI-MS m/z: 554.1 $[M - Cl]^+$. IR (KBr): 3788, 3060, 1604, 1543, 1470, 1409, 1291, 1271, 1217, 1163, 1098, 1073, 1047, 1015, 910, 787, 757, 681, 428 cm^{-1}. Elemental analysis calcd (%) for $C_{24}H_{23}Cl_2N_3O_2RuS$: C 48.90, H 3.93, N 7.13; found: C 48.85, H 3.97, N 7.09.

*Data for **Ru5**.* The black block crystals were suitable for structural characterization. Yield (0.0568 g, 93.20%). ESI-MS m/z: 652.2 $[M - Cl + DMSO]^+$. ^{1}H NMR (600 MHz, DMSO-d_6) δ 9.44–9.38 (m, 2H), 8.89 (s, 2H), 8.70 (d, J = 8.0 Hz, 2H), 8.18–8.13 (m, 2H), 7.97 (ddd, J = 7.7, 3.6, 1.4 Hz, 3H), 7.84 (dd, J = 7.0, 0.9 Hz, 1H), 7.77 (dd, J = 8.1, 7.2 Hz, 1H), 7.69–7.64 (m,

2H), 7.57–7.52 (m, 2H), 2.54 (s, 6H). ^{13}C NMR (151 MHz, DMSO-d_6) δ 158.82, 157.01, 155.72, 147.96, 136.84, 136.08, 133.41, 130.41, 129.42, 128.65, 127.81, 127.42, 126.47, 125.65, 124.74, 123.49, 122.49, 40.42, 39.92, 39.78, 39.65, 39.51, 39.37, 39.23, 39.09. IR (KBr): 3854, 3444, 3054, 2361, 1630, 1605, 1541, 1480, 1416, 1388, 1240, 1160, 1065, 1046, 1015, 790, 677, 633, 539, 429 cm^{-1}. Elemental analysis calcd (%) for $C_{27}H_{23}Cl_2N_3ORuS$: C 53.20, H 3.80, N 6.89; found: C 53.16, H 3.85, N 6.87.

*Data for **Ru6**.* The black product of **Ru6** was suitable for structural characterization. Yield (0.0542 g, 79.30%). ESI-MS *m*/*z*: 726.2 [M − Cl + DMSO]$^+$. ^{1}H NMR (600 MHz, DMSO-d_6) δ 9.47–9.42 (m, 2H), 9.03 (s, 2H), 8.74 (d, J = 8.1 Hz, 2H), 8.55 (d, J = 7.8 Hz, 1H), 8.42 (d, J = 7.6 Hz, 1H), 8.38 (dd, J = 7.6, 4.1 Hz, 2H), 8.35–8.33 (m, 2H), 8.30 (d, J = 16.2 Hz, 2H), 8.17 (t, J = 7.6 Hz, 1H), 8.01–7.96 (m, 2H), 7.60–7.56 (m, 2H), 3.67 (s, 3H), 2.54 (s, 6H). ^{13}C NMR (151 MHz, DMSO-d_6) δ 158.88, 157.08, 155.79, 148.25, 136.86, 133.32, 131.41, 130.92, 130.37, 128.91, 128.39, 127.95, 127.35, 126.77, 126.51, 126.01, 125.58, 125.08, 124.09, 123.88, 123.55, 122.92, 44.63, 40.43, 39.94, 39.80, 39.66, 39.52, 39.38, 39.24, 39.10. IR (KBr): 3751, 3445, 3046, 2361, 1603, 1584, 1565, 1468, 1400, 1316, 1048, 1016, 846, 791, 722, 681, 657, 563 cm^{-1}. Elemental analysis calcd (%) for $C_{33}H_{25}Cl_2N_3ORuS$: C 57.98, H 3.69, N 6.15; found: C 57.96, H 3.75, N 6.12.

Materials, instrumentation, and the experimental methods. Tris, RNase A, and propidium iodide (PI) were purchased from Sigma. The hTERT, β-actin, and c-myc antibodies were purchased from Abcam. The EGFP (enhanced green fluorescent protein) and c-myc gene vectors, total RNA isolation kit, and two-step RT-PCR kit were purchased from TIANGEN. All the human cell lines (BEL-7404, Hep-G2, NCI-H460, MGC80-3, and HL-7702 cells) were obtained from the Shanghai Institute for Biological Science (China). ct-DNA and other DNA oligomers (highly polymerized stored at 4 °C and long-term storage at −20 °C) are listed in Table S7† and were obtained from Shanghai Sangon Biological Engineering Technology & Services (Shanghai, China). Stock solutions of all the compounds (2 mM) were made in DMSO, and further dilutions to working concentrations were made with the corresponding buffer. The X-ray crystallography structure of **Ru5** was solved with direct methods and refined using the SHELX-97 program.[76,77] The materials, instrumentation, RT-PCR, cytotoxicity assay, cellular morphology, RNA extraction, uptake of Ru in Hep-G2 cells, cell apoptosis, western blot, and transfection assay of **Ru1**–**Ru6** were performed as reported by Chao, Reed, Liang, and Chen.[8,20,32,71,72,78,79]

Conflicts of interest

The authors declare no competing interest.

Acknowledgements

This work was supported by the National Natural Science Foundation of China (No. 21261025, 21761033), the Key Foundation Project of Colleges and Universities in Guangxi (No. ZD2014108), the Innovative Team & Outstanding Talent Program of Colleges and Universities in Guangxi (2014-49 and 2017-38), the PhD Research Startup Program of Yulin Normal University (No. G2017009), IRT_16R15, the project of Guibei characteristic medicine resources research center of Guangxi Province (KYA201703), the basic skills improvement project for the young and middle-aged teachers in Guangxi colleges and universities (KY2016YB595), the Yulin Normal University Research Grant (2018YJKY34 and 2015YJYB08), as well as the State Key Laboratory for the Chemistry and Molecular Engineering of Medicinal Resources, Ministry of Science and Technology of China (CMEMR2017-B17 and CMEMR2014-B08).

Notes and references

1 A. T. Phan, V. Kuryavyi, H. Y. Gaw and D. J. Patel, *Nat. Chem. Biol.*, 2005, **1**, 167–173.
2 A. T. Phan, V. Kuryavyi, S. Burge, S. Neidle and D. J. Patel, *J. Am. Chem. Soc.*, 2007, **129**, 4386–4392.
3 P. S. Shirude, B. Okoumus, L. Ying, T. Ha and S. Balasubramanian, *J. Am. Chem. Soc.*, 2007, **129**, 7484–7485.
4 A. K. Todd, S. M. Haider, G. N. Parkinson and S. Neidle, *Nucleic Acids Res.*, 2007, **35**, 5799–5808.
5 J. Dai, T. S. Dexheimer, D. Chen, M. Carver, A. Ambrus, R. A. Jones and D. Yang, *J. Am. Chem. Soc.*, 2006, **128**, 1096–1098.
6 T. S. Dexheimer, D. Sun and L. H. Hurley, *J. Am. Chem. Soc.*, 2006, **128**, 5404–5415.
7 L. Yuan, T. Tian, Y. Chen, S. Yan, X. Xing, Z. Zhang, Q. Zhai, L. Xu, S. Wang, X. Weng, B. Yuan, Y. Feng and X. Zhou, *Sci. Rep.*, 2013, **3**, 1811.
8 Q. P. Qin, J. L. Qin, T. Meng, G. A. Yang, Z. Z. Wei, Y. C. Liu, H. Liang and Z. F. Chen, *Sci. Rep.*, 2016, **6**, 37644.
9 T. M. Ou, Y. J. Lu, C. Zhang, Z. S. Huang, X. D. Wang, J. H. Tan, Y. Chen, D. L. Ma, K. Y. Wong, J. C. O. Tang, A. S. C. Chan and L. Q. Gu, *J. Med. Chem.*, 2007, **50**, 1465–1474.
10 T. Simonsson, M. Pribylova and M. Vorlickova, *Biochem. Biophys. Res. Commun.*, 2000, **278**, 158–166.
11 E. H. Postel, S. J. Berberich, J. W. Rooney and D. M. Kaetzel, *J. Bioenerg. Biomembr.*, 2000, **32**, 277–284.
12 T. Simonsson, P. Pecinka and M. Kubista, *Nucleic Acids Res.*, 1998, **26**, 1167–1172.
13 P. Wu, D. L. Ma, C. H. Leung, S. C. Yan, N. Zhu, R. Abagyan and C. M. Che, *Chem. – Eur. J.*, 2009, **15**, 13008–13021.
14 T. Lemarteleur, D. Gomez, R. Paterski, E. Mandine, P. Mailliet and J. F. Riou, *Biochem. Biophys. Res. Commun.*, 2004, **323**, 802–808.
15 C. L. Grand, H. Han, R. M. MuÇoz, S. Weitman, D. D. Von Hoff, L. H. Hurley and D. J. Bearss, *Mol. Cancer Ther.*, 2002, **1**, 565–573.
16 J. Seenisamy, S. Bashyam, V. Gokhale, H. Vankayalapati, D. Sun, A. Siddiqui-Jain, N. Streiner, K. Shin-ya, E. White, W. D. Wilson and L. H. Hurley, *J. Am. Chem. Soc.*, 2005, **127**, 2944–2959.
17 Y. J. Lu, T. M. Ou, J. H. Tan, J. Q. Hou, W. Y. Shao, D. Peng, N. Sun, X. D. Wang, W. B. Wu, X. Z. Bu, Z. S. Huang, D. L.

Ma, K. Y. Wong and L. Q. Gu, *J. Med. Chem.*, 2008, **51**, 6381–6392.
18 Y. Ma, T. M. Ou, J. Q. Hou, Y. J. Lu, J. H. Tan, L. Q. Gu and Z. S. Huang, *Bioorg. Med. Chem.*, 2008, **16**, 7582–7591.
19 A. Rangan, O. Y. Fedoroff and L. H. Hurley, *J. Biol. Chem.*, 2001, **276**, 4640–4646.
20 J. E. Reed, A. A. Arnal, S. Neidle and R. Vilar, *J. Am. Chem. Soc.*, 2006, **128**, 5992–5993.
21 C. Zhao, J. Ren, Y. Xu and X. Qu, *J. Am. Chem. Soc.*, 2013, **135**, 18786–18789.
22 R. Kieltyka, J. Fakhoury, N. Moitessier and H. F. Sleiman, *Chem. – Eur. J.*, 2008, **14**, 1145–1154.
23 A. De Cian, E. DeLemos, J. L. Mergny, M. P. Teulade-Fichou and D. Monchaud, *J. Am. Chem. Soc.*, 2007, **129**, 1856–1857.
24 R. Kieltyka, P. Englebienne, J. Fakhoury, C. Autexier, N. Moitessier and H. F. Sleiman, *J. Am. Chem. Soc.*, 2008, **130**, 10040–10041.
25 D. L. Ma, C. M. Che and S. C. Yan, *J. Am. Chem. Soc.*, 2009, **131**, 1835–1846.
26 J. R. Choudhury, R. Guddneppanavar, G. Saluta, G. L. Kucera and U. Bierbach, *J. Med. Chem.*, 2008, **51**, 3069–3072.
27 J. Zhu, Y. Zhao, Y. Zhu, Z. Wu, M. Lin, W. He, Y. Wang, G. Chen, L. Dong, J. Zhang, Y. Lu and Z. Guo, *Chem. – Eur. J.*, 2009, **15**, 5245–5253.
28 X. H. Zheng, Y. F. Zhong, C. P. Tan, L. N. Ji and Z. W. Mao, *Dalton Trans.*, 2012, **42**, 11807–11812.
29 V. Viglasky, *Rev. Geophys.*, 2009, **276**, 401–409.
30 J. Wang, K. Lu, S. Xuan, Z. Toh, D. Zhang and F. Shao, *Chem. Commun.*, 2013, **49**, 4758–4760.
31 E. Largy, F. Hamon, F. Rosu, V. Gabelica, E. D. Pauw, A. Guedin, J. L. Mergny and M. P. Teulade-Fichou, *Chem. – Eur. J.*, 2011, **17**, 13274–13283.
32 C. Wang, Q. Yu, L. Yang, Y. Liu, D. Sun, Y. Huang, Y. Zhou, Q. Zhang and J. Liu, *BioMetals*, 2013, **26**, 387–402.
33 M. J. Li, T. Y. Lan, Z. S. Lin, C. Yi and G. N. Chen, *J. Biol. Inorg. Chem.*, 2013, **18**, 993–1003.
34 S. T. Von, H. L. Seng, H. B. Lee, S. W. Ng, Y. Kitamura, M. Chikira and C. H. Ng, *J. Biol. Inorg. Chem.*, 2012, **17**, 57–69.
35 Q. Cao, Y. Li, E. Freisinger, P. Z. Qin, R. K. O. Sigel and Z. W. Mao, *Inorg. Chem. Front.*, 2017, **4**, 10–32.
36 H. Bertrand, D. Monchaud, A. De Cian, R. Guillot, J. L. Mergny and M. P. Teulade-Fichou, *Org. Biomol. Chem.*, 2007, **5**, 2555–2559.
37 P. Wang, C. H. Leung, D. L. Ma, S. C. Yan and C. M. Che, *Chem. – Eur. J.*, 2010, **16**, 6900–6911.
38 S. Gama, I. Rodrigues, F. Mendes, I. C. Santos, E. Gabano, B. Klejevskaja, J. Gonzalez-Garcia, M. Ravera, R. Vilar and A. Paulo, *J. Inorg. Biochem.*, 2016, **160**, 275–286.
39 C. Wei, L. Ren and N. Gao, *Int. J. Biol. Macromol.*, 2013, **57**, 1–8.
40 K. Suntharalingam, A. J. P. White and R. Vilar, *Inorg. Chem.*, 2009, **48**, 9427–9435.
41 J. T. Wang, Y. Li, J. H. Tan, L. N. Ji and Z. W. Mao, *Dalton Trans.*, 2011, **40**, 564–566.
42 C. Yu, K. H. Y. Chan, K. M. C. Wong and V. W. W. Yam, *Chem. Commun.*, 2009, 3756–3758.
43 D. L. Ang, B. W. J. Harper, L. Cubo, O. Mendoza, R. Vilar and J. Aldrich-Wright, *Chem. – Eur. J.*, 2016, **22**, 2317–2325.
44 K. Suntharalingam, A. J. P. White and R. Vilar, *Inorg. Chem.*, 2010, **49**, 8371–8380.
45 V. S. Stafford, K. Suntharalingam, A. Shivalingam, A. J. P. White, D. J. Mann and R. Vilar, *Dalton Trans.*, 2015, **44**, 3686–3700.
46 M. N. Patel, D. S. Gandhi, P. A. Parmar and H. N. Joshi, *J. Coord. Chem.*, 2012, **65**, 1926–1936.
47 M. N. Patel, P. A. Parmar, D. S. Gandhi and V. R. Thakkar, *Inorg. Chem. Commun.*, 2010, **13**, 1480–1484.
48 D. Roberto, F. Tessore, R. Ugo, S. Bruni, A. Manfredi and S. Quici, *Chem. Commun.*, 2002, 846–847.
49 F. Tessore, D. Roberto, R. Ugo and M. Pizzotti, *Inorg. Chem.*, 2005, **44**, 8967–8978.
50 K. K. Patel, E. A. Plummer, M. Darwish, A. Rodger and M. J. Hannon, *J. Inorg. Biochem.*, 2002, **91**, 220–229.
51 D. Mondal, S. Biswas, A. Paul and S. Baitalik, *Inorg. Chem.*, 2017, **56**, 7624–7641.
52 D. Maity, C. Bhaumik, D. Mondal and S. Baitalik, *Inorg. Chem.*, 2013, **52**, 13941–13955.
53 Y. Li, M. Cheng, J. Hao, C. Wang, G. Jia and C. Li, *Chem. Sci.*, 2015, **6**, 5578–5585.
54 H. Y. Zhou, F. Q. Dong, X. L. Du, Z. K. Zhou, H. R. Huo, W. H. Wang, H. D. Zhan, Y. F. Dai, J. Meng, Y. P. Sui, J. Li, F. Sui and Y. H. Zhai, *Bioorg. Med. Chem. Lett.*, 2016, **26**, 3876–3880.
55 Q. P. Qin, T. Meng, Z. Z. Wei, C. H. Zhang, Y. C. Liu, H. Liang and Z. F. Chen, *Eur. J. Inorg. Chem.*, 2017, **2017**, 1824–1834.
56 X. B. Fu, D. D. Liu, Y. Lin, W. Hu, Z. W. Mao and X. Y. Le, *Dalton Trans.*, 2014, **43**, 8721–8737.
57 R. Cao, J. L. Jia, X. C. Ma, M. Zhou and H. Fei, *J. Med. Chem.*, 2013, **56**, 3636–3644.
58 J. L. Qin, Q. P. Qin, Z. Z. Wei, C. C. Yu, T. Meng, C. X. Wu, Y. L. Liang, H. Liang and Z. F. Chen, *Eur. J. Med. Chem.*, 2016, **124**, 417–427.
59 E. Schreiber, P. Matthias, M. M. Mueller and W. Schaffner, *Nucleic Acids Res.*, 1989, **17**, 6419.
60 I. Romero-Canelón, A. M. Pizarro, A. Habtemariam and P. J. Sadler, *Metallomics*, 2012, **4**, 1271–1279.
61 T. Meng, S. F. Tang, Q. P. Qin, Y. L. Liang, C. X. Wu, C. Y. Wang, H. T. Yan, J. X. Dong and Y. C. Liu, *Med. Chem. Commun.*, 2016, **7**, 1802–1811.
62 Y. Xia, Q. Chen, X. Qin, D. Sun, J. Zhang and J. Liu, *New J. Chem.*, 2013, **37**, 3706–3715.
63 X. Chen, J. H. Wu, Y. W. Lai, R. Zhao, H. Chao and L. N. Ji, *Dalton Trans.*, 2013, **42**, 4386–4397.
64 D. Sun, R. Zhang, F. Yuan, D. Liu, Y. Zhou and J. Liu, *Dalton Trans.*, 2012, **41**, 1734–1741.
65 V. Casagrande, E. Salvati, A. Alvino, A. Bianco, A. Ciammaichella, C. D'Angelo, L. Ginnari-Satriani, A. M. Serrilli, S. Iachettini, C. Leonetti, S. Neidle, G. Ortaggi, M. Porru, A. Rizzo, M. Franceschin and A. Biroccio, *J. Med. Chem.*, 2011, **54**, 1140–1156.
66 Q. Yu, Y. Liu, J. Zhang, F. Yang, D. Sun, D. Liu, Y. Zhou and J. Liu, *Metallomics*, 2013, **5**, 222–231.

67 O. Domarco, D. Lötsch, J. Schreiber, C. Dinhof, S. Van Schoonhoven, M. D. García, C. Peinador, B. K. Keppler, W. Berger and A. Terenzi, *Dalton Trans.*, 2017, **46**, 329–332.
68 R. Martí-Centelles, J. Murga, E. Falomir, M. Carda and J. A. Marco, *Med. Chem. Commun.*, 2015, **6**, 1809–1815.
69 A. Terenzi, R. Bonsignore, A. Spinello, C. Gentile, A. Martorana, C. Ducani, B. Högberg, A. M. Almerico, A. Lauria and G. Barone, *RSC Adv.*, 2014, **4**, 33245–33256.
70 Y. Zhao, D. Cheng, S. Wang and J. Zhu, *Nucleic Acids Res.*, 2014, **42**, 10385–10398.
71 Q. P. Qin, J. L. Qin, T. Meng, W. H. Lin, C. H. Zhang, Z. Z. Wei, J. N. Chen, Y. C. Liu, H. Liang and Z. F. Chen, *Eur. J. Med. Chem.*, 2016, **124**, 380–392.
72 Z. F. Chen, Q. P. Qin, J. L. Qin, J. Zhou, Y. L. Li, N. Li, Y. C. Liu and H. Liang, *J. Med. Chem.*, 2015, **58**, 4771–4789.
73 M. Chalfie, Y. Tu, G. Euskirchen, W. W. Ward and D. C. Prasher, *Science*, 1994, **263**, 802–805.
74 T. C. He, A. B. Sparks, C. Rago, H. Hermeking, L. Zawel, L. T. da Costa, P. J. Morin, B. Vogelstein and K. W. Kinzler, *Science*, 1998, **281**, 1509–1512.
75 G. B. Jiang, J. H. Yao, J. Wang, W. Li, B. J. Han, Y. Y. Xie, G. J. Lin, H. L. Huang and Y. J. Liu, *New J. Chem.*, 2014, **38**, 2554–2563.
76 G. M. Sheldrick, *SHELXTL-97, Program for refinement of crystal structures*, University of Göttingen, Germany, 1997.
77 G. M. Sheldrick, *SHELXS-97, Program for solution of crystal structures*, University of Göttingen, Germany, 1997.
78 L. Xu, X. Chen, J. Wu, J. Wang, L. Ji and H. Chao, *Chem. – Eur. J.*, 2015, **21**, 4008–4020.
79 Q. P. Qin, T. Meng, M. X. Tan, Y. C. Liu, X. J. Luo, B. Q. Zou and H. Liang, *Eur. J. Med. Chem.*, 2018, **143**, 1387–1395.